Jurnal Teknologi

Full Paper

WIDEBAND JEAN ANTENNA WITH BENDING STRUCTURE FOR MICROWAVE IMAGING APPLICATIONS

Roshayati Yahya[a,b], Muhammad Ramlee Kamarudin[b*], Norhudah Seman[b], Ali Moradikordalivand[b]

[a]Faculty of Electrical and Electronics, University Tun Hussein Onn Malaysia, Parit Raja, 86400 Batu Pahat, Johor, Malaysia
[b]Wireless Communication Centre (WCC), Universiti Teknologi Malaysia, 81310 UTM Johor Bahru, Johor, Malaysia

Article history
Received
23 June 2015
Received in revised form
14 November 2015
Accepted
23 January 2015

*Corresponding author
ramlee@fke.utm.my

Graphical abstract

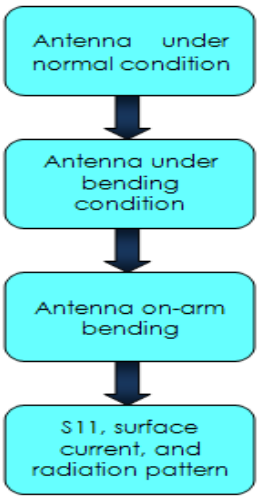

Abstract

In this paper, a wideband jean antenna with bending structure for flexible microwave imaging applications is presented. Coplanar waveguide (CPW) feeding structure with Koch shape ground slotted technique has been implemented for widening the bandwidth. The design evolution process of the proposed antenna is started from a simple CPW-fed monopole antenna to bending circumstance. The proposed antennas under normal condition, bending circumstance and as well as on-arm bending effect are simulated and optimized using CST microwave studio software and fabricated; also tested so as to validate the results . Under normal condition, the antenna provides measured bandwidth of 4500 MHz (1.5–6 GHz) in the case of $|S11| \leq -10$ dB while 4360 MHz (1.44–5.8 GHz) for the measured bandwidth under bending circumstance is obtained. Also, there is a slight degradation on the reflection coefficient of the antenna under on-arm bending so that measured bandwidth became narrower with operating frequency of 3800 MHz (2.2–6 GHz). The measured gain of the antenna fluctuates between 2.5–5.6 dBi and 1.5–2.8 dBi with quasi-omnidirectional pattern within the expected frequency band for normal and bending condition, respectively. The proposed antenna provides a good performance in terms of its reflection coefficient and radiation characteristics. Therefore, due to insensitiveness to bending and body effect, the proposed antenna has become good candidate for microwave imaging applications.

Keywords: Wideband antenna; textile antenna; microwave imaging

1.0 INTRODUCTION

Antenna is an integral component in communication systems. The possibility of implementing wideband antenna is highly advantageous including weight reduction, reduced fabrication costs, smaller installation area, and reduction in electromagnetic compatibility issue [1]. Wideband antennas are extensively used as premier parts for data interpretation and analysis [2]in various fields; for instances, satellite communications, wireless applications[3-5], and the currently proposed in microwave imaging field [6-8].

There are countless numbers of wideband microstrip antennas have been proposed for microwave imaging system. One of them is antenna in [9] that purposely design for breast imaging. The antenna is fabricated on FR4 substrate with overall dimension of 100×100×100 mm^3 and can be only fit the regular breast size. Therefore, scanning process cannot be performed for the samples which cannot fit the dimension. Hence, more prototyping cost is needed for different sizes of breast samples. There is almost similar limitation occurred for head imaging setup proposed in [10]. The array of antennas is designed specifically for head. The antenna that constructed by Rogers RO3010 is integrated into other mechanical parts to form an array for facilitating the scanning process. However, more spaces are needed to accommodate the device, besides the antenna can

be only used for head scanning. On the other hand, the proposed imaging antennas have limitations of their implementation on different and various sizes, shapes, and body parts. Moreover, the curvy structure of the human body is also important to be considered.

Due to limitations of the substrate used in the previous imaging system, this study proposes more flexible substrate compared to printed circuit board. Therefore, by emphasizing the flexibility and robust bending capability which is not achievable in any of the counterpart microstrip antennas, textile antenna is seen to be the best option. Thus, this flexible material is able to be applied on any part of human body regardless hand, chest, breast, or head using the same antenna. Moreover, textile antenna provides further advantages due to its light weight, ease of integration with clothes, and low cost. Besides, textile antennas can be easily sewn, whereas sewing is not possible with the microstrip antennas. Therefore, the research that is carried out in this study provides the investigations on the antenna's characteristics under bending condition. In addition, the performance of the textile antenna on real human arm is also presented.

2.0 ANTENNA DESIGN EVOLUTION

According to the requirement on a flexible material, a fully textile antenna which constructed from jean substrate has been proposed. The antenna has been designed and simulated in Computer Simulation Technology (CST) software. Dielectric constant values, ε_r of jean substrate are presented in Figure 1. According to the Figure 1, ε_r of jean is obviously much lower than FR4. On the contrary, *tan δ* of jean is larger than FR4. This is due to the FR4 is definitely created for electronic circuit and devices. Consequently, the substrate is manufactured with the intention to have very low loss values. Instead, jean fabric for clothing is targeted to provide comfort to the wearer without taking into account the losses. However, this study performs investigations on the antenna design and performance of using non-technical-material of jean as the substrate. The radiating elements (patch and ground) are designed and fabricated on polyester taffeta fabric (also known as pure copper fabric) with resistivity 0.05 Ohm/sq and thickness of 0.08 mm.

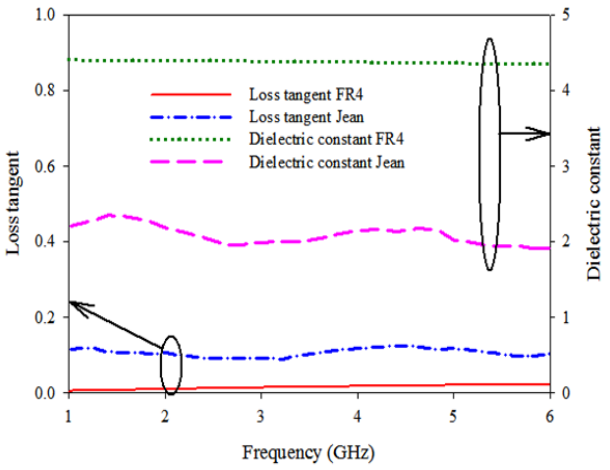

Figure 1 Dielectric constant (ε_r) and loss tangent (*tan δ*) of FR4 and jean substrate

Based on ε_r values throughout the frequency range, all the values are uploaded in the simulator to monitor the changes of the antenna performance. According to [11], ground plane of a microstrip patch antenna has insignificant effect if the thickness of its substrate is very large. Therefore, it can be removed, so that the structure becomes similar to a monopole antenna. Thus, many researches have been conducted to constitute monopole antenna as a typical structure of microstrip patch antenna. Therefore, width, w_p of the radiating patch is initially designed according to rectangular microstrip patch antenna equation in [12] as shown in (1).

$$w_p = \frac{1}{2f_r\sqrt{\mu_0\,\varepsilon_0}}\sqrt{\frac{2}{\varepsilon_r+1}} \quad (1)$$

The resonance frequency, $f_r$is taken as 3.5 GHz with ε_r= 2.25 at the selected frequency. The formula to calculate the length, $l_p$of the radiating patch is indicated in (2).

$$l_p = \frac{1}{2f_r\sqrt{\varepsilon_{reff}}\sqrt{\mu_0\,\varepsilon_0}} - 2\Delta L \quad (2)$$

The effective dielectric constant, $\varepsilon_{reff}$and extension of the length, ΔL is given by (3) and (4) respectively.

$$\varepsilon_{reff} = \frac{\varepsilon_r+1}{2} + \frac{\varepsilon_r-1}{2}\left[1+12\frac{h}{W_p}\right]^{-1/2} \quad (3)$$

$$\frac{\Delta L}{h} = 0.412\frac{(\varepsilon_{reff}+0.3)\left(\frac{W_p}{h}+0.264\right)}{(\varepsilon_{reff}-0.258)\left(\frac{W_p}{h}+0.8\right)} \quad (4)$$

Figure 2(a)-(d) describes the steps on designing the antenna. The calculated w_p and l_p of radiating patch is 34 mm and 28 mm accordingly, while the dimensions of the antenna are performed in Table 1. The ground is designed with square slot of l_k = 44 mm, and another

similar square is rotated 90° to perform the Koch slot as shown in Figure 2(d).

In addition, the simulated views of the antenna under bending and on-arm bending conditions are presented in respected to Figure 3(a) and (b). The bending performance of the antenna is simulated on Polyvinyl Chloride (PVC) that has ε_r=2.8 [13], curving radius of 40 mm, and thickness of 1.6 mm. The PVC has been used for bending support due to the antenna cannot be bent independently on air with any specific radius as shown in Figure 3(a).Nevertheless, the simulation on the antenna performance with the presence of the human body (on-arm bending) is also performed. Five layers geometry of the human arm is modeled in the simulator by concentric cylinders with a radius of 50 mm. The layers representing the thicknesses of the tissues of skin (1.5 mm), fat (8.5 mm), muscle (27.5 mm), cortical bone (6 mm), and bone marrow (6.5 mm) as described in Figure 3(b)[14].

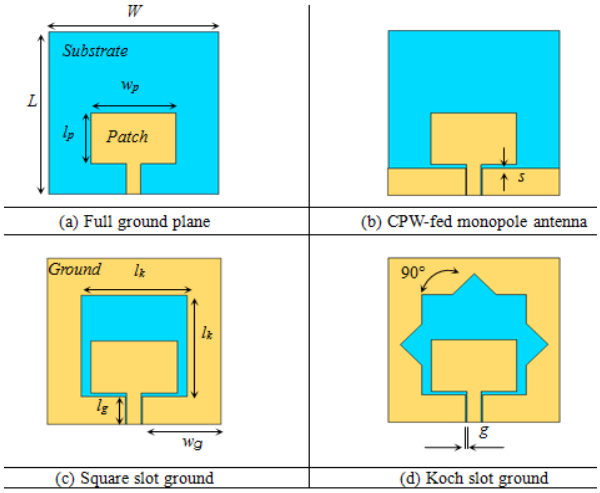

Figure 2 Steps in designing the antenna

Table 1 Antenna parameters and dimensions

Item	Dimension (mm)
L	72
W	72
wp	34
lp	28
lk	44
lg	11.5
wg	32.5
g	0.5 ± 0.1
s	1.5

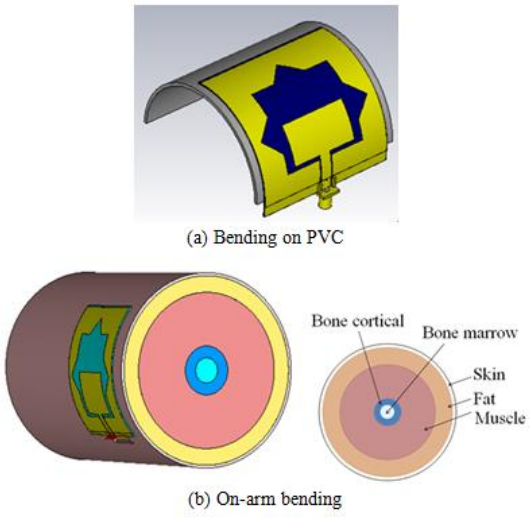

Figure 3 Bending illustrations on PVC and on-arm

3.0 FABRICATION AND MEASUREMENT

Radiating element parts of the antenna are printed on a piece of paper that later is pasted on the pure copper fabric using double sided tape. Both of the paper and pure copper fabric are manually cut using scissor. The radiating elements are then attached to the jean substrate by using hand-sewn technique. It should be noted here that a conductive thread is used for sewing the antenna. The prototype of the antenna is presented in Figure 4(a). The antenna is then attached to PVC using double sided tape as in Figure 4(b), while in-arm band is done using masking tape as shown in Figure 4(c).

In this study, an Agilent Network Analyzer E5071C is used to measure the reflection coefficient while the radiation pattern is measured in an anechoic chamber. The antenna is firstly observed in the under normal condition, which its prototype stands upright during the measurement process. The strapping structure of the jean makes the textile could stand with no support requirement. On the other hand, antenna under bending condition and with the presence of the human body is discovered. In body communication system, it has been proven that the characteristics of antennas have been affected by the presence of the human body [15,16]. As earlier mentioned, the measurement of antenna radiation patterns under normal and bending condition have been done in an anechoic chamber. However, the radiation pattern measurement of on-arm bending cannot be done due to radiation, health, and safety factor. Results of |S11| and the radiation pattern of the antenna are discussed in the next section.

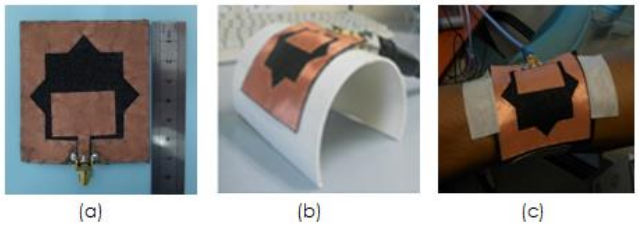

Figure 4 Antenna under three different conditions. **(a)** Normal condition,**(b)** Under bending circumstance, and **(c)** On-arm bending

4.0 RESULTS AND DISCUSSIONS

Scattering parameter (|S11|), surface current distribution and radiation patterns of the antenna under three conditions (normal, bending, and on-arm bending) are performed in this section.

4.1 Scattering Parameter

Comparison on |S11| for the antenna design evolution is presented in Figure 5. According to the |S11| of the antenna while having the full ground plane, the antenna provides the bandwidth of 350 MHz (3.6–3.95 GHz) base on the |S11|≤−10 dB. In addition, the bandwidth of the antenna with the CPW-fed partial ground is increased, which covers bandwidth of 2530 MHz (1.97–4.5 GHz). However, while taking into account the bending formation for microwave imaging, directive antenna should be considered. As is well known, directive antenna is related to full ground plane microstrip antenna which limits the ability to obtain the antenna with large bandwidth. Therefore, ground slot technique has been introduced towards the wide bandwidth aim. Even though the square slot minimizes the impedance bandwidth; the implementation of rotated square (Koch slot) has obviously expanded the impedance bandwidth of 4750MHz (1.25–6 GHz).

The |S11| of simulated and measured result of the antenna under three circumstances are compared in Figure 6. In normal condition, the simulated |S11|covers 1.25–6 GHz (4750 MHz) while measured |S11| provides 1.5- 6 GHz (4500 MHz) with experimented fractional BW of 1.2 or 120%. This percentage indicates wideband characteristic of the antenna under normal condition. Compared to [17] less bandwidth is covered due to the Koch technique. This shows that, by using lower ε_r substrate of jean, the bandwidth can be improved [18].

Simulated and measured |S11| of the antenna under bending circumstance are also presented in Figure 6. The simulated and measured |S11| under bending circumstance operates at 1.22–6 GHz (4780 MHz) and 1.44–5.8 GHz (4360 MHz), respectively. Similar experimented fractional BW has been obtained of the bending antenna to the antenna under normal condition which is 1.2 or 120%.

Nevertheless, simulated |S11| of the antenna while it is bent on arm operates at 1.75–6 GHz (4250 MHz), while the measured |S11| works at 2.2–6 GHz (3800 MHz). The measured fractional BW of 0.93 or 93 % is obtained. This indicates that the |S11| of on-arm bending antenna may narrow the bandwidth due to the presence of human body effect. There is also slight deviation between simulated and measured results due to the numerical arm used homogeneous part, whilst real human arm

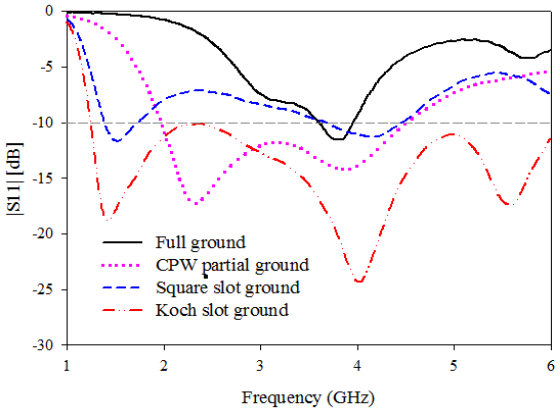

Figure 5 |S11| of antenna design evolution

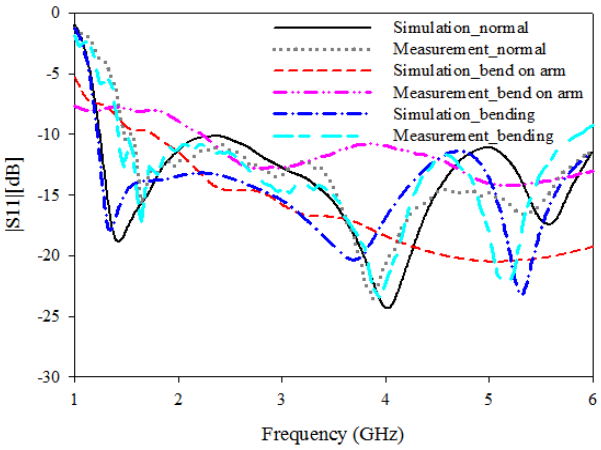

Figure 6 Simulated and measured |S11| of the antenna under normal, bending, and on-arm bending

consists of inhomogeneous part, for instance, nerves, blood, and skin pores. Performance of the antenna due to body effect is difficult to be estimated due to body absorption, movement and shadowing effect that could contribute more losses and will degrade the antenna performances. However, the effect of on-arm bending towards the proposed antenna gives reasonable and acceptable results.

4.2 Surface Current Distributions

Surface current shows the electric field distribution of the antenna. Referring to Figure 7, there were the depictions of simulated current distribution of the

antenna under normal, bending, and on-arm bending condition at 2, 4, and 6 GHz. It can be observed that, surface current at 2 GHz under normal condition has longer path on the edge of the patch and on the inner side of the Koch ground. Meanwhile, the distribution of electric field decreases at 4 and 6 GHz, where the current path is the shortest at 6 GHz. Moreover, surface current under bending condition concentrated on the lower part of the patch and ground at 2 GHz, with longer path of current than 4 and 6 GHz. At 4 GHz, the current is focused on the top, and re-concentrated at the lower part of the antenna at 6 GHz.In contrast, the on-arm bending antenna has longer current path on the sides of the patch and the triangular ground shape at 2 GHz. However, shorter current path focused on the bottom part of the patch at 4 and 6 GHz. According to the results of surface current, the length of the current path presents the wavelength that generated by the antenna. Thus, the longer the current path shows the longer of wavelength that generates lower resonance of frequency, and vice versa.

In addition, it can be also observed that, the electric field strength is concentrated on the feed of the antenna at most frequencies, instead of on the Koch slotted ground. Therefore, these show that the Koch ground plays an important role in electrical field distribution throughout the frequency bandwidth regardless under normal, bending, or on-arm bending.

4.3 Radiation Characteristics

The simulated and measured radiation patterns of antenna under normal, bending, and on-arm bending condition at 2 and 4 GHz are shown in Figure 8. It can be seen that simulated and measured E-plane demonstrates a bi-directional radiation pattern; while H-plane shows a nearly omni-directional radiation pattern for both 2 and 4 GHz under normal condition. However, there is nearly omni-direction for all simulated and measured E-plane and H-plane of the antenna at 2 and 4 GHz under bending circumstance. Moreover, there is slightly shift about 30° of the E-plane radiation pattern of both 2 and 4 GHz compared to normal condition. The shift angle occurs due to the bending effect of the antenna. Based on the Figure 8, it can be seen that there is good agreement between simulated and measured radiation patterns of the antenna in the normal and bending condition.

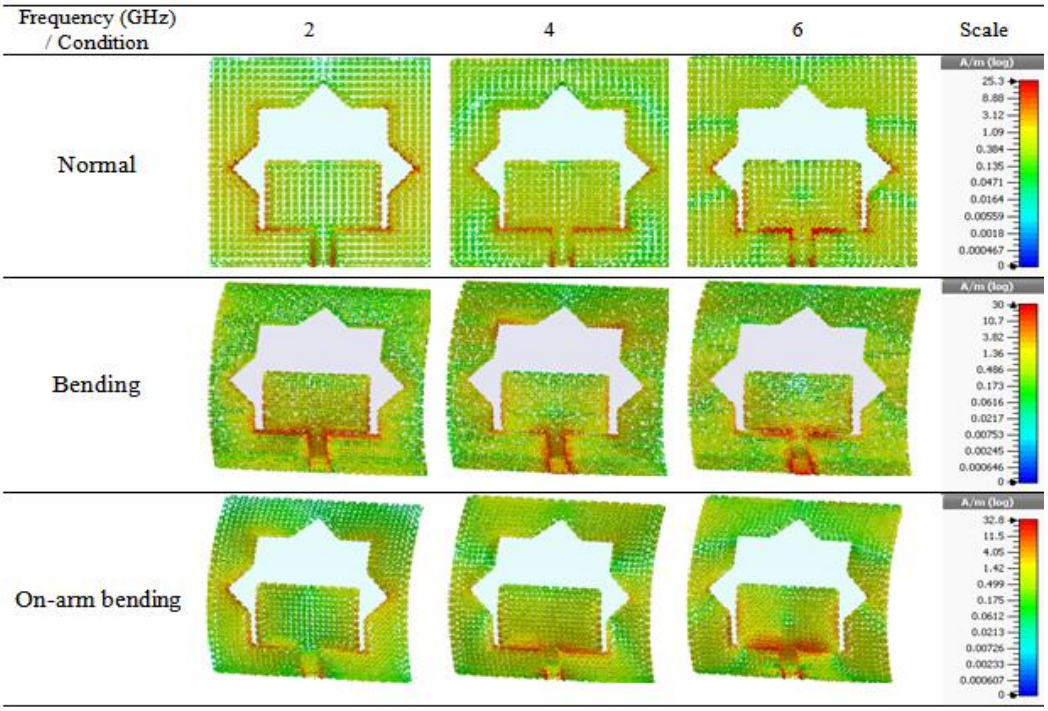

Figure 7 Simulated surface current distribution of the antenna under normal, bending, and on-arm condition

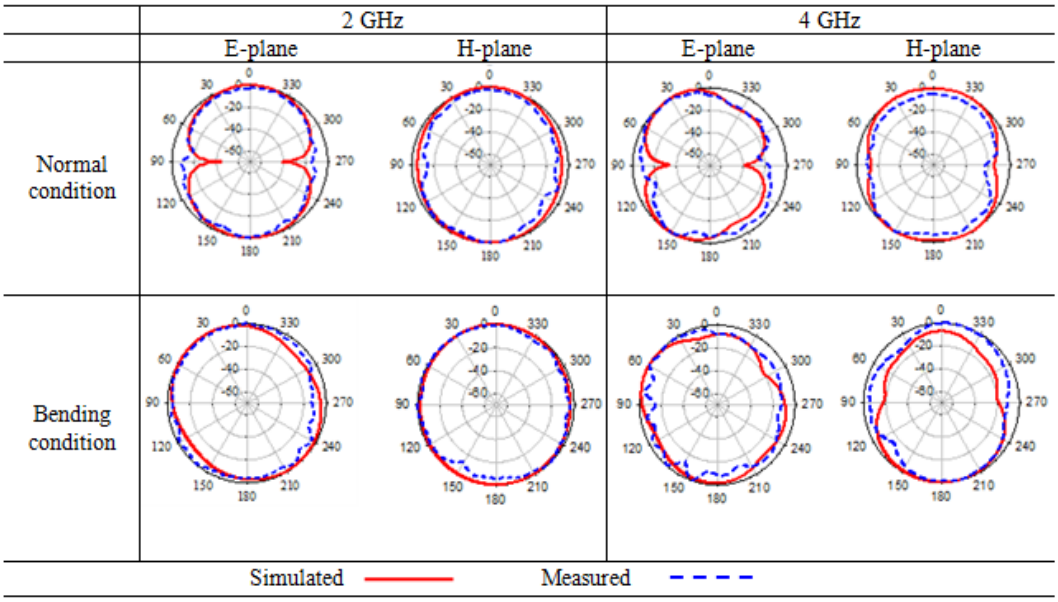

Figure 8 Radiation patterns of the antenna under normal and bending conditions at 2 and 4 GHz

Measured gain and simulated efficiency results of the antenna under normal and bending condition are shown in Figure 9. On-arm bending antenna is not measured in the chamber due to radiation and safety factors. As can be observed in Figure 9, measured gain of the antenna under normal condition increases proportionally to the frequency increment from 2 to 5 GHz, except at 6 GHz. The gain value fluctuates from 2.5–5.6 dBi throughout the frequency band. Subsequently, the gain of the antenna under bending circumstance provides lower gain compared to the gain under normal condition with fluctuating values of 1.5–2.8 dBi at 2–6 GHz. The gain increases from 2–4 GHz and decreasing for the frequency higher than 4 GHz. It can be seen that; gain of the antenna under bending decreases near 50 % compared to the normal condition.

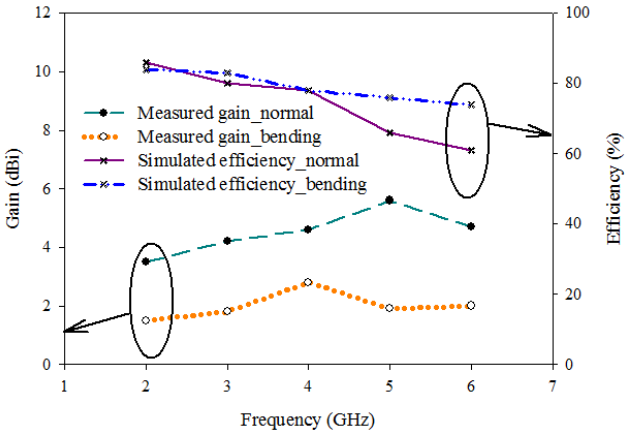

Figure 9 Measured gain and simulated efficiency of the antenna under normal and bending condition

According to the simulated efficicency, the values are decreasing proportional to the frequency increment. The efficiencies of the antenna decreases from 86–61 % and 84–74 % for the condition of normal and under bending circumstances, accordingly. Nevertheless, the efficiency of the antenna under normal condition shows rapid decrement at higher frequency, while there is only 10 % reduction between 2 GHz and 6 GHz for the bending condition. It shows that the antenna under bending condition is less affect to the efficiency.

5.0 CONCLUSION

The investigations on jean antenna for microwave imaging application have been studied and presented in this paper. The CPW-fed structure with the Koch slot on the ground is implemented to increase the impedance bandwidth. There are good agreements between simulated and measured |S11| under normal, bending, and on-arm bending condition for |S11|≤−10 dB. The measured fractional bandwidth of 120% (1.5–6 GHz), 120% (1.44–5.8 GHz), and 93% (2.2–6 GHz) has been obtained according to the antenna under normal, bending, and on-arm bending. Also, the measured gains of the antenna are obtained more than 2.5 dBi in normal condition and 1.5 dBi in bending condition. In addition, a nearly omnidirectional pattern within the expected frequency band is achieved for both normal and bending condition. These results show that the antenna has a wideband characteristic which is a potential candidate for microwave imaging application due to the insensitiveness to bending and insignificant effect on the presence of the human body.

Acknowledgement

The authors would like to thank the Ministry of Science, Technology and Innovation (MOSTI) under Science Fund (Vote 4S056), Ministry of Education (MOE) and UTM for funding this project under GUP Grant (Vote 05H34 and Vote 00M69). Nevertheless, special thank you to UTHM for sponsoring the first author to embark on this research.

References

[1] Guraliuc, A. R., Caso, R., Nepa, P., and Volakis, J. L. 2012. Numerical Analysis of a Wideband Thick Archimedean Spiral Antenna, *IEEE Antennas Wireless Propagation Letters*.11: 168–171.

[2] Che, R. and Seman, N. 2013. Reflection Coefficient Measurement through the Implementation of Wideband Multi - Port Reflectometer with Error Correction for Microwave Imaging Application of Human Head. *Jurnal Teknologi*. 6(3): 7–13.

[3] Ramirez, M. and Parron, J. 2012. Concentric Annular Ring Slot Antenna for Global Navigation Satellite Systems. *IEEE Antennas Wireless Propagation Letters*. 11: 705–707.

[4] Khidre, A., Lee, K., Yang, F., and Elsherbeni, A. Z. 2013. Circular Polarization Reconfigurable Wideband E-Shaped Patch Antenna for Wireless Applications. *IEEE Transaction on Antennas and Propagation*. 61(2): 260–263.

[5] Wong, H. S., Islam, M. T., and Kibria, S. 2014. Design and Optimization of LTE 1800 MIMO Antenna. *Scientific World Journal*. 725806.

[6] Kharkovsky, S., Ghasr, M. T., Kam, K., Abou-Khousa, M. a., and Zoughi, R. 2013. Out-of-Plane Fed Elliptical Slot Array for Microwave Imaging. *IEEE Transaction on Antennas and Propag*ation. 61(10): 5311–5314.

[7] Bourqui, J., Okoniewski, M., and Fear, E. C. 2010. Balanced Antipodal Vivaldi Antenna With Dielectric Director for Near-Field Microwave Imaging. *IEEE Transaction on Antennas and Propag*ation. 58(7): 2318–2326.

[8] Hafiz, M., Rahiman, F., Tan, T., Kiat, W., Ping, S., and Abdul, R. 2015. Microwave Tomography Application and Approaches – A Review. *Jurnal Teknologi*. 73(3): 133–138.

[9] Yu, J., Yuan, M., and Liu, Q. H. 2009. A Wideband Half Oval Patch Antenna for Breast Imaging. *Progress In Electromagnetics Research*. 98: 1–13.

[10] Mohammed, B. J., Abbosh, A. M., Mustafa, S. and Ireland, D. 2014.Microwave System for Head Imaging. *IEEE ransactions on Instrumentation and Measurement*. 63(1): 117–123.

[11] Ray, K. and Anob, P. 2001. Broadband Planar Rectangular Monopole Antennas. *Microwave and Optical Technology Letters*. 28(1): 55–59.

[12] Balanis, C. A. 2005. Antenna Theory: Analysis and Design. Second Edition. *Wiley*.

[13] Jarvis, J. B., Janezic, M. D., Riddle, B. F., Johnk, R. T., Kabos, P., Geyer, C. L. H. R. G., and Grosvenor, C. A. 2005. Measuring the Permittivity and Permeability of Lossy Materials: Solids, Liquids, Metals, Building Materials, and Negative-Index Materials. *National Institute of Standards and Technology*.

[14] Wegmueller, M. and Kuhn, A. 2007. An attempt to Model the Human Body as a Communication Channel. *IEEE Transactions on Bio-medical Engineering*. 54(10): 1851–1857.

[15] Kamarudin, M. R. and Hall, P. 2009. Diversity Performance of Body Communication Channels Using Switching Parasitic Disk-loaded Monopole Array Antenna. *Microwave and Optical Technology Letters*. 51(5): 1157–1161.

[16] Kamarudin, M. R., Nechayev, Y. I., and Hall, P. S. 2009. Onbody Diversity and Angle-of-Arrival Measurement Using a Pattern Switching Antenna.*IEEE Transactions on Antennas and Propagation*. 57(4): 964–971.

[17] Zhang, H., Xu H.Y., Tian, B., and Zeng, X.-F. 2012. Cpw-fed Fractal Slot Antenna for UWB Application.*International Journal of Antennas and Propagation*. 2012: 1–4.

[18] Rao, N. and Kumar, V. D. 2011. Gain and Bandwidth Enhancement of a Microstrip Antenna Using Partial Substrate Removal in Multiple-layer Dielectric Substrate. *PIER Proceedings*. 1285–1289.